

Driven harmonic oscillator as a quantum simulator for open systems

Jyrki Piilo and Sabrina Maniscalco

Department of Physics, University of Turku, FI-20014 Turun yliopisto, Finland

(Dated: February 1, 2008)

We show theoretically how a driven harmonic oscillator can be used as a quantum simulator for the non-Markovian damped harmonic oscillator. In the general framework, our results demonstrate the possibility to use a closed system as a simulator for open quantum systems. The quantum simulator is based on sets of controlled drives of the closed harmonic oscillator with appropriately tailored electric field pulses. The non-Markovian dynamics of the damped harmonic oscillator is obtained by using the information about the spectral density of the open system when averaging over the drives of the closed oscillator. We consider single trapped ions as a specific physical implementation of the simulator, and we show how the simulator approach reveals new physical insight into the open system dynamics, e.g. the characteristic quantum mechanical non-Markovian oscillatory behavior of the energy of the damped oscillator, usually obtained by the non-Lindblad-type master equation, can have a simple semiclassical interpretation.

PACS numbers: 03.67.Lx, 03.65.Yz, 32.80.Pj

I. INTRODUCTION

Recent years have witnessed a considerable experimental and theoretical progress in quantum information science [1, 2, 3]. A major factor for the rapid development has been the increasing ability to control and engineer the quantum states of single and few particle systems. The development of the field is expected to continue in fast pace and some applications, e.g. for quantum cryptography, are already commercially available. One of the most active contemporary subfields of quantum information science and of nanotechnology is the study of quantum simulators [3, 4, 5, 6, 7, 8].

Simulating quantum systems by classical computers remains a challenging task due to the inherent inability of classical systems to incorporate the quantum features in an efficient way. The development of quantum simulators, i.e. a controllable quantum system imitating the behavior of other quantum systems of interest, holds the promise for a generation of powerful means and devices to study quantum systems and provides additional ways to gain new insight into their peculiar quantum features.

A notable aspect of recent proposals for quantum simulators is their ability to cross the usual boundaries between different fields of physics [6, 7, 8], e.g. a certain configuration of cold atoms trapped in optical lattices has been recently proposed to simulate superstrings [8]. These, as well as more “conservative” quantum simulators [4, 5], are often based on cold trapped atoms and gases because of the recently developed abilities to manipulate their properties in an extremely precise way.

In this paper we develop a quantum simulator scheme for open quantum systems exploiting the recent progress in trapped ion technologies [9]. The motivation to develop quantum simulators for open systems stems especially from their central role in the progress towards fault-tolerant quantum information processing. Indeed, decoherence, which is a key issue for successful quantum gate implementation, is a topic typically studied in terms

of open quantum systems [10].

We focus on a quantum simulator scheme for a damped harmonic oscillator which is a paradigmatic model of open quantum systems [10] and has a wide variety of applications ranging, e.g., from quantum optics [11] and nuclear physics [12] to chemistry [13]. We show how a driven harmonic oscillator can be used to mimic the behavior of the damped harmonic oscillator. In other words, we demonstrate theoretically the possibility to use a closed system as a quantum simulator for open quantum system.

Our quantum simulator is based on the controlled driving of a closed harmonic oscillator by sets of appropriately tailored electric fields. We show how the sets of drives in different frequency regimes give rise to various types of dynamical features of the driven oscillator, and how these shed light on the effects that the various parts of the environment spectrum have on the open system dynamics to be simulated. The total non-Markovian dynamics of the damped harmonic oscillator is obtained by using the information about the spectral density of the open system when averaging over the sets of drives of the closed oscillator.

A well known example of experimental realization of quantum harmonic oscillator is a single trapped ion [9] and we discuss the implementation of the simulator with this system. The effects of random electromagnetic fields on the trapped ion dynamics has been recently studied [14, 15, 16]. In the usual approaches, the system dynamics is calculated averaging over known stochastic properties of the environment fields. Our approach is taken from the opposite direction. We ask if it is possible to drive the closed oscillator in a controlled way so that the effect mimics the open system dynamics. Our results highlight the possibility to simulate artificial, engineered reservoirs, by controlled sets of drives. In general, reservoir engineering is emerging as an active contemporary research topic for the control and the fundamental study of open quantum systems [17, 18, 19, 20].

The quantum simulator approach, already at a theoretical level, makes it possible to gain new insight into the complex non-Markovian dynamics of the damped oscillator. The simulator approach allows to identify the origin of the different dynamical features of the non-Markovian dynamics of the open system and sheds light on the role that the phase of the random environmental fields plays in the system dynamics. Furthermore we show how the implementation of the quantum simulator with a trapped ion allows to interpret a typical quantum mechanical behavior, usually described with a non-Lindblad-type master equation, by semiclassical means. We also discuss the implications of the quantum simulator approach towards the continuous measurement scheme interpretation of the quantum trajectories for non-Markovian open systems [21].

The paper is organized as follows. Section II introduces the model of a closed harmonic oscillator driven by controlled fields and sets the framework for the quantum simulator approach presented in Sec. III. Here, the damped oscillator model to be simulated, is presented, and we furthermore discuss the new insight that the simulator approach brings to light. Section IV shows how the quantum simulator can be implemented with a trapped ion and the discussion concludes the paper in Sec. V.

II. DRIVEN OSCILLATOR DYNAMICS

A. The basic scheme: pulsed driving

We begin by considering the dynamics of a closed quantum harmonic oscillator which is driven by a single frequency field for a set of runs which we label by the frequency ω of the field. In each run of the set ω , the duration of the applied field changes. In other words, a single set of runs with frequency ω consists of drives with increasing duration of the pulses mapping the oscillator dynamics as a function of time. The frequency of the driving field changes for different sets of runs and depends on the type of the environment and spectral density to be simulated.

It is important to emphasize that the dynamics of the closed oscillator is not monitored (measured) in a continuous way. Rather, the scheme for a single run of the set ω can be summarized as follows: (i) Switch on the driving field at time $t_1 = 0$. The state of the oscillator may change suddenly due to a sudden switch on of the driving field. (ii) Driving of the oscillator with external field of frequency ω for $0 < t < t_2$. (iii) Switch off of the driving field at $t = t_2$. The state of the oscillator may change suddenly due to a sudden switch off of the driving field. With the set of pulses, with increasing t_2 for the members of the set ω , one maps the oscillator dynamics. The key ingredient for the simulator, for the system we study, is related to the effects of switching on and off of the field.

The Hamiltonian of a quantum harmonic oscillator

driven by a time dependent periodic force is [22]

$$H = \hbar\omega_0 \left(a^\dagger a + \frac{1}{2} \right) + \hbar F(t)(a + a^\dagger). \quad (1)$$

Here, ω_0 is the frequency of the oscillator, a^\dagger (a) is the creation (annihilation) operator of the energy quanta of the oscillator, and the periodic driving force is

$$F(t) = \frac{A \cos(\omega t + \varphi)}{\sqrt{2m\hbar\omega_0}}, \quad (2)$$

where A describes the amplitude and ω the oscillation frequency of the periodic force, m is the mass of the oscillator, and φ is the phase of the driving field.

B. Off-resonant driving

We assume, for simplicity, that the oscillator is initially in the ground state. In this case it can be shown that the heating function $\langle n \rangle = \langle a^\dagger a \rangle$, for $\omega \neq \omega_0$, can be written

$$\begin{aligned} \langle n \rangle(t, \omega) = & |\alpha|^2 \left[\left(\frac{\omega}{\omega_0} \right)^2 - 1 \right]^{-2} \left[1 + \cos^2(\omega t) \right. \\ & - 2 \cos(\omega t) \cos(\omega_0 t) - 2 \frac{\omega}{\omega_0} \sin(\omega t) \sin(\omega_0 t) \\ & \left. + \left(\frac{\omega}{\omega_0} \right)^2 \sin^2(\omega t) \right], \end{aligned} \quad (3)$$

where the phase of the field is chosen for convenience $\varphi = 0$ and $\alpha = A/\sqrt{2m\hbar\omega_0}$.

Figures 1 (a), (b), and (c) show examples of the time evolutions of $\langle n \rangle$ for $\omega/\omega_0 = 0.0, 0.1, 0.2$. In the following two subsections we discuss in detail the heating function dynamics for constant field drive ($\omega = 0$) and in the adiabatic regime ($\omega \ll \omega_0$). In these frequency ranges, the dynamical features of the driven oscillator heating function allow to gain interesting insight into the non-Markovian dynamics of the open system (to be discussed in Sec. III).

1. Constant field

When driving the system with a constant field $\omega = 0$, the heating function displays sinusoidal oscillations, see Fig. 1 (a). This can be explained in the following way: (i) Switching on the driving field at time $t_1 = 0$. A suddenly switched on constant force displaces the ground state of the oscillator creating a coherent state $D(\alpha)|0\rangle = |\alpha\rangle$ (ii) Time evolution between $t_1 < t < t_2$. The coherent state oscillates in the trap according to the free evolution (no change in $\langle n \rangle$). (iii) Switching off the field at $t = t_2$. The initial displacement of (i) is reversed $[D(-\alpha)]$. Moreover, the effect of the second displacement depends on the phase of the oscillation of the coherent state.

The final state of the system at time t_2 (after the second displacement) is

$$|\psi(t)\rangle = |-\alpha + \alpha \exp(-i\omega_0 t)\rangle, \quad (4)$$

and the heating function becomes

$$\langle n \rangle(t) = |-\alpha + \alpha \exp(-i\omega_0 t)|^2 = 2|\alpha|^2(1 - \cos \omega_0 t). \quad (5)$$

The second displacement brings the coherent state back to the ground state after full oscillation periods whereas half the period of oscillation of the coherent state during $t_1 < t < t_2$ causes a total displacement of 2α . The heating function consequently oscillates between 0 and $4|\alpha|^2$. Setting $\omega = 0$ in the general result of Eq. (3) matches the simple result [Eq. (5)] and confirms this interpretation.

2. Driving with small frequency in adiabatic regime

Let us consider now the case $0 < \omega \ll \omega_0$. Since the driving frequency is much smaller than the oscillator frequency, the oscillator follows adiabatically the changes of the force. Figures 1 (b) and (c) display examples of drivings in this regime for $\omega/\omega_0 = 0.1, 0.2$.

Also here, the switches on and off of the drive field are thought to happen instantaneously compared to the oscillator dynamics. The simple scheme of the previous subsection is replaced with: (i) Switching on the field at time $t_1 = 0$. As before, the switched on field displaces the ground state of the oscillator creating a coherent state $D(\alpha)|0\rangle = |\alpha\rangle$ (ii) Time evolution between $t_1 < t < t_2$. The coherent state oscillates in the trap according to the free evolution (no change in $\langle n \rangle$). Moreover, the periodic driving force with frequency ω changes slowly. The oscillator follows adiabatically the consequent slow motion of the oscillator center since $\omega_c \ll \omega_0$. (iii) Switching off the field at $t = t_2$. Because of the slow oscillation of the driving force, the magnitude of the second displacement depends now also on driving frequency ω and on time t : $D(-\cos(\omega t) \exp(-i\omega_0 t)\alpha)$.

Following this scheme, the state of the oscillator after the second displacement can be written

$$|\psi(t)\rangle = |e^{-i\omega_0 t}\alpha - \cos(\omega t)\alpha\rangle, \quad (6)$$

and the heating function becomes

$$\langle n \rangle(t, \omega) = |\alpha|^2 [1 + \cos^2(\omega t) - 2 \cos(\omega t) \cos(\omega_0 t)]. \quad (7)$$

This matches the general result of Eq. (3) when the terms containing $\omega/\omega_0 \ll 1$ are neglected (adiabatic limit) and confirms the interpretation presented here.

C. On resonant driving

The equation (3) for the heating function is not well defined for $\omega = \omega_0$. Beginning from the Hamiltonian

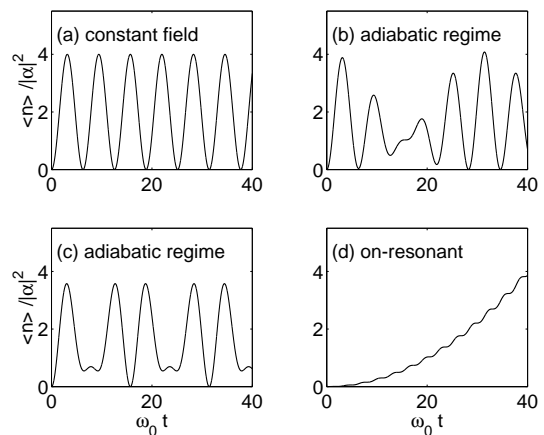


FIG. 1: Time evolution of the heating function of the closed driven oscillator in three different frequency regimes for four different driving frequencies: (a) $\omega/\omega_0 = 0$, (b) $\omega/\omega_0 = 0.1$, (c) $\omega/\omega_0 = 0.2$, (d) $\omega/\omega_0 = 1.0$. Please note that we have multiplied the result in (d) by a factor of 0.01 (a weight factor given by the spectral density we use in Sec. III).

of Eq. (1) one can show that on-resonant driving of the oscillator gives for the heating function (for convenience the phase of the field is set $\varphi = 0$)

$$\langle n \rangle(t, \omega_0) = \frac{1}{4}|\alpha|^2 [\omega_0^2 t^2 + \omega_0 t \sin(2\omega_0 t) + \sin^2(\omega_0 t)]. \quad (8)$$

Figure 1 (d) displays an example of the heating function dynamics in this case. We note that the oscillatory terms play a minor role contrary to the off-resonant constant field and adiabatic cases.

III. DRIVEN OSCILLATOR AS A QUANTUM SIMULATOR

In the previous section we have shown the main dynamical features of the pulsed driven oscillator in various frequency ranges of the driving force (constant force, adiabatic regime, on-resonant driving). We show now that by combining the dominant dynamical features from the three main frequency regimes, one can construct a quantum simulator for an open quantum system. We begin by recalling the basic features of the system to be simulated.

A. System to be simulated: damped harmonic oscillator

The damped harmonic oscillator is one of the paradigmatic models used to describe the dynamics of open quantum systems [10]. We briefly recall the form of the master equation for the reduced system density matrix which allows to describe the non-Markovian dynamics of the damped oscillator. For a more detailed presentation, see e.g. Ref. [23] and references therein.

The dynamics of a harmonic oscillator linearly coupled to a quantized reservoir, modelled as an infinite chain of quantum harmonic oscillators, is described, in the secular approximation, by means of the following generalized master equation [23, 24]

$$\begin{aligned} \frac{d\rho(t)}{dt} = & \frac{\Delta(t) + \gamma(t)}{2} [2a\rho(t)a^\dagger - a^\dagger a\rho(t) - \rho(t)a^\dagger a] \\ & + \frac{\Delta(t) - \gamma(t)}{2} [2a^\dagger \rho(t)a - aa^\dagger \rho(t) - \rho(t)aa^\dagger], \end{aligned} \quad (9)$$

with $\rho(t)$ the reduced density matrix of the system harmonic oscillator. The time dependent coefficients $\Delta(t)$ and $\gamma(t)$ appearing in the master equation are known as diffusion and dissipation coefficients, respectively [23, 24].

The diffusion coefficient for high temperature reservoir $k_B T / \omega_0 \gg 1$ and to second order in the dimensionless coupling constant g , can be written [23, 25]

$$\begin{aligned} \Delta(t) = & 2g^2 k_B T \frac{r^2}{1+r^2} \{1 - e^{-\omega_c t} [\cos(\omega_0 t) \\ & - (1/r) \sin(\omega_0 t)]\}. \end{aligned} \quad (10)$$

Above, $r = \omega_c / \omega_0$ is the ratio between the environment cut-off frequency ω_c and the oscillator frequency ω_0 , k_B is the Boltzmann constant, and T is the temperature. For the high temperature case the dissipation coefficient $\gamma \ll \Delta$ and therefore is neglected.

A typical environment of open systems is described by an Ohmic reservoir spectral density with Lorentz-Drude cut-off [26]

$$J(\omega) = \frac{2\omega}{\pi} \frac{\omega_c^2}{\omega_c^2 + \omega^2}, \quad (11)$$

for a schematic view, see Fig. 2. The spectral distribution is given by

$$\begin{aligned} I(\omega) = & J(\omega)[n_e(\omega) + 1/2] \\ = & \frac{\omega}{\pi} \frac{\omega_c^2}{\omega_c^2 + \omega^2} \coth(\omega/KT), \end{aligned} \quad (12)$$

where $n_e(\omega)$ is the population of the environment mode of frequency ω , and Eq. (11) has been used. For high T , Eq. (12) becomes

$$I(\omega) = \frac{2k_B T}{\pi} \frac{\omega_c^2}{\omega_c^2 + \omega^2}. \quad (13)$$

The central parameter $r = \omega_c / \omega_0$ describes how on-resonant the oscillator is with the reservoir. When $r > 1$, intensive part of the environment spectrum overlaps with the oscillator frequency and the decay coefficient $\Delta(t) > 0$ for all times. Consequently, the master equation is of Lindblad-type. When $r < 1$ (Fig. 2), the most intense part of the environment spectrum lies in small frequency range and the on-resonant intensity is small. In this case

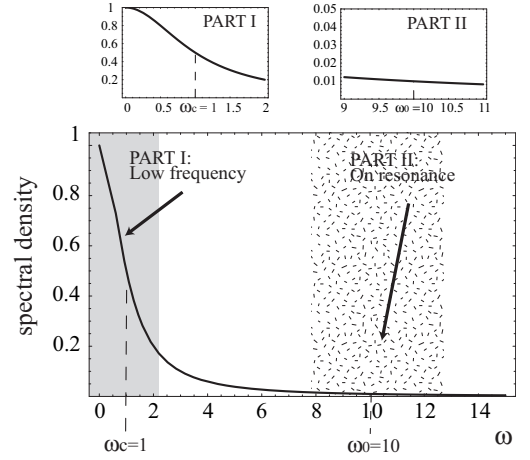


FIG. 2: Schematic view of the spectral density and the splitting of the spectrum ($r = 0.1$). Part I is the low frequency part which produces the sudden displacements of the oscillator state when switching on and off. Part II is the on-resonant part which produces Markovian type heating.

the decay coefficient $\Delta(t)$ acquire temporarily negative values and the master equation is of non-Lindblad-type [23].

The full solution of the the master equation (9) can be found, e.g., in Refs. [23, 27]. For an initial Fock state $|n = 0\rangle$ it turns out that, in the secular approximation, the state of the system at each time t is a thermal state with “effective” temperature changing in time according to the behavior of $\langle n(t) \rangle$ (see Appendix A):

$$\rho_{k,k} = \left[\frac{\langle n(t) \rangle}{\langle n(t) \rangle + 1} \right]^k \frac{1}{\langle n(t) \rangle + 1}. \quad (14)$$

It is worth emphasizing that the short time non-Markovian effects are described by the non-monotonic changes in $\langle n \rangle$ [see the exact result for $\langle n \rangle$ in Fig. 3 (d)]. The non-Markovian regime is then followed by Markovian linear heating and finally for long times the system reaches a steady state in thermal equilibrium with its environment (see Ref. [28] for a discussion of the origin of the oscillations of the heating function in the non-Markovian regime and Ref. [29] for a discussion of the Markovian and thermalization regimes).

It is also possible to see from the master equation (9) that for an initial Fock state the coherences vanish for all times in the Fock-state basis. This is due to the fact that the equations of motions for the diagonal elements $\rho_{k,k}(t)$ and off-diagonal elements $\rho_{k,k'}(t)$, with $k \neq k'$, decouple. In particular this means that the equations of motion for the off-diagonal elements $\rho_{k,k'}(t)$, do not depend on the diagonal elements $\rho_{k,k}(t)$. Since for an initial Fock state $\rho_{k,k'}(0) = \langle k | \rho(0) | k' \rangle = 0$, the decoupling then implies that $\rho_{k,k'}(t) = 0$ for all t and $k \neq k'$.

For an initial ground state in the weak coupling ($\langle n(t) \rangle \ll 1$) and for times much shorter than the ther-

malization time one obtains

$$\begin{aligned}\rho_{0,0} &= \frac{1}{\langle n(t) \rangle + 1} \simeq 1 - \langle n(t) \rangle \\ \rho_{1,1} &\simeq \langle n(t) \rangle.\end{aligned}\quad (15)$$

The analytic solution for the heating function and for $\langle n(0) \rangle = 0$ is given by [23]

$$\langle n(t) \rangle = \int_0^t \Delta(t') dt', \quad (16)$$

where $\Delta(t)$ has been given in Eq. (10). The exact heating function dynamics, given by Eq. (16), will be used as a benchmark for the theoretical quantum simulator results in the following subsection.

B. Simulating damped harmonic oscillator with driven oscillator

We have calculated in Sec. II the heating function dynamics for a driven oscillator. The oscillator is driven

with single frequency fields in a pulsed way, the frequencies covering the relevant part of the environment spectrum of the damped oscillator. We now proceed to show how the complete damped harmonic oscillator dynamics is recovered when the information about the spectral density is used to average the driven oscillator results. We first demonstrate that the simulator gives correct heating function dynamics and then present the complete solution showing that the density matrices of the simulator and of the damped harmonic oscillator match.

1. Heating function

Equation (3) describes the heating function for off-resonant driving with $\varphi = 0$. When the phase of the driving field is taken into account, the heating function can be written

$$\begin{aligned}\langle n \rangle(t, \omega, \varphi) &= |\alpha|^2 \left[\left(\frac{\omega}{\omega_0} \right)^2 - 1 \right]^{-2} \left\{ \cos^2(\varphi) + \cos^2(\omega t + \varphi) - 2 \cos(\varphi) \cos(\omega t + \varphi) \cos(\omega_0 t) - 2 \frac{\omega}{\omega_0} \sin(\omega t) \sin(\omega_0 t) \right. \\ &\quad \left. - 2 \left(\frac{\omega}{\omega_0} \right)^2 \sin(\varphi) \sin(\omega t + \varphi) \cos(\omega_0 t) + \left(\frac{\omega}{\omega_0} \right)^2 [\sin^2(\varphi) + \sin^2(\omega t + \varphi)] \right\}.\end{aligned}\quad (17)$$

To obtain the final result, we average Eq. (17) over the phase of the driving field and over the various driving frequencies by using the spectral density as a weight factor

$$\langle n \rangle(t) = \frac{1}{N} \int_0^\infty d\omega \frac{1}{2\pi} \int_0^{2\pi} d\varphi I(\omega) \langle n \rangle(t, \omega, \varphi). \quad (18)$$

Averaging over the phase gives,

$$\begin{aligned}\langle n \rangle(t) &= \frac{|\alpha|^2}{N} \int_0^\infty d\omega I(\omega) \left[1 - \left(\frac{\omega}{\omega_0} \right)^2 \right]^{-2} \\ &\quad \times \left\{ \left[1 + \left(\frac{\omega}{\omega_0} \right)^2 \right] [1 - \cos(\omega_0 t) \cos(\omega t)] \right. \\ &\quad \left. - 2 \frac{\omega}{\omega_0} \sin(\omega t) \sin(\omega_0 t) \right\},\end{aligned}\quad (19)$$

where N is the normalization factor. We average also over the frequency, and thus the normalizing factor, in the case we consider, becomes

$$N = \omega_c \frac{2}{\pi} \int_0^\infty d\omega \frac{\omega_c^2}{\omega_c^2 + \omega^2} = \omega_c^2. \quad (20)$$

We obtain the result for the heating function dynamics of a damped oscillator by plugging in the spectral distribution [Eq. (13)], into the phase averaged result, Eq. (19). In the regime $r < 1$ the non-Lindblad-type dynamics dominates. The environment is detuned from the system frequency, the most intense part of the environment appears for small frequencies $\omega \ll \omega_0$ whereas the on-resonant part corresponds to the low intensity part of the spectral density. We set the parameters as follows: $r = 0.1$, $g = 0.045$, $k_B/\omega_0 = 80$.

The results from single frequency drives [Figs. 1 (a)-(c)] suggest that the low frequency part of the spectrum (part I in Fig. 2) induces oscillations of the heating function. In contrast, the result for $\omega = \omega_0$ [Fig. 1 (d)] indicates that the near-resonant part of the environment spectrum (part II in Fig. 2), produces a Markovian-type heating.

Indeed, when we calculate the result by integrating over the low frequency part, $0 \leq \omega/\omega_0 \leq 0.2$, the heating function displays damped oscillations, see Fig. 3 (a). When the result is calculated by integrating over the on-resonant part, $0.8 \leq \omega/\omega_0 \leq 1.2$, the heating function displays linear dynamics, see Fig. 3 (b). When we add these two results obtained by integrating over the limited

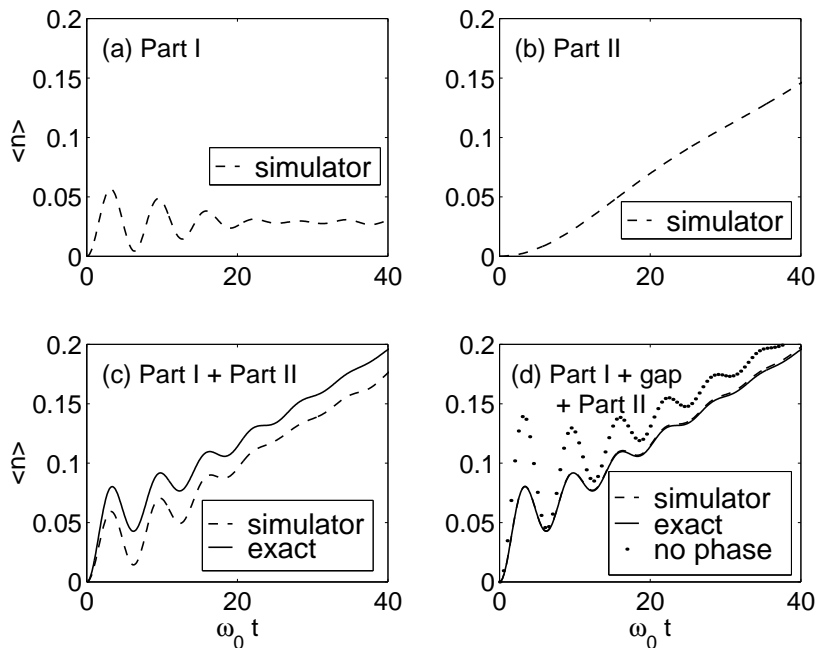


FIG. 3: Comparison between the quantum simulator and the exact results for the non-Markovian oscillatory dynamics. The results demonstrate how the different parts of the environment spectrum affect the dynamics. (a) $0 \leq \omega/\omega_0 \leq 0.2$, (b) $0.8 \leq \omega/\omega_0 \leq 1.2$, (c) $0.0 \leq \omega/\omega_0 \leq 0.2$ and $0.8 \leq \omega/\omega_0 \leq 1.2$, (d) $0.0 \leq \omega/\omega_0 \leq 1.2$. Moreover, the results in (d) show how the random phase of the driving field influences the amplitude of the oscillations of the heating function. Due to the excellent match between the simulator and the exact results in (d), it is difficult to see any difference between the two.

frequency range, the heating function displays the dominant characteristics of the exact result and the match between the two results is already quite close, see Fig. 3 (c). If we then add to the integration the gap between the two frequency regimes presented above, the match between the quantum simulator and the exact results is excellent and it becomes difficult to see any difference between the two, see Fig. 3 (d).

These results illustrate how we can identify the origin of the dominating features of the heating function dynamics in the various parts of the environment spectrum. It is also worth noting that the simulator result in Fig. 3 (d) includes the non-adiabatic effects, which are not contained in the simple result of Fig. 3 (c). Obviously, the inclusion of the non-adiabatic effects enhances the match giving excellent agreement between the quantum simulator and the exact results. Moreover, according to the simple displacement scheme for single frequency drives (presented in the previous section), the damping of the heating function oscillations arises in a subtle way as an indirect consequence of several low frequencies involved. All the low frequencies involved affect the simulator dynamics in a similar way when the driving field is switched on. However, the effect of the second displacement, when the field is switched off, depends on the frequency and it consequently damps the oscillations.

We have also checked the agreement between the exact and quantum simulator results for the typical quadratic non-Markovian regime ($r \sim 10$) and for a Markovian

regime ($r > 20$, $t \gg 1/\omega_c$). For a fundamental theoretical study of various types of dynamics see Ref. [23].

It is also interesting to study the case where the phase of the driving field is kept fixed. This illuminates an aspect about the effect of the random phase of the environmental noise being simulated. The result for the fixed-phase, $\varphi = 0$, is displayed in Fig. 3 (d), dotted line. The random phase does not seem to play a role for Markovian heating since the slope of the linear increase in $\langle n \rangle$ for large times is the same for the fixed phase and for the phase averaged results. Instead, the phases of the low frequency fields affect the short time oscillatory behavior of the heating function by influencing the amplitude of the oscillation. Without averaging over the phase, and setting $\varphi = 0$, gives larger oscillations as can be seen in Fig. 3 (d). When studying the Markovian case ($r > 20$), we noticed, that the fixed phase and random phase results very closely agree. This indicates again that the random phase plays a significant role only in the non-Markovian dynamics.

2. Density matrix

So far we have demonstrated that the averaged driven oscillator results can mimic correctly the heating function dynamics of the open system. It remains to be shown that actually the simulated density matrix matches the density matrix of the non-Markovian damped harmonic

oscillator, given by Eq. (14).

The single frequency drive (see Eq. (1) for the Hamiltonian) creates a coherent state. Following Ref. [22] and using the complex field representation of the driving force, it can be shown that the amplitude of the coherent state, for driving field frequency ω and phase φ , is given by

$$\begin{aligned} \beta(t, \omega, \varphi) = & -\kappa \left\{ \frac{e^{-i\varphi}}{\frac{\omega}{\omega_0} + 1} [e^{i\omega_0 t} - e^{-i\omega t}] \right. \\ & \left. + \frac{e^{i\varphi}}{\frac{\omega}{\omega_0} - 1} [e^{i\omega t} - e^{i\omega_0 t}] \right\}, \end{aligned} \quad (21)$$

where the dimensionless coupling constant κ is

$$\kappa = \frac{A}{\sqrt{2m\hbar\omega_0^3}}. \quad (22)$$

The matrix elements in the Fock-state basis are given in the usual way

$$\rho_{k,l}(t, \omega, \varphi) = e^{-|\beta|^2} \frac{\beta^k \beta^{*l}}{\sqrt{k!l!}} = e^{-|\beta|^2} \frac{\beta^{k-l} |\beta|^{2l}}{\sqrt{k!l!}}. \quad (23)$$

We recall that the analytic result for the damped harmonic oscillator is valid for weak couplings. To compare the results, we expand the exponential in Eq. (23) and keep the terms to second order in the dimensionless coupling constant κ . For the sake of simplicity we consider here the case of an initial state $|n=0\rangle$ but the results can be generalized in a straightforward way to other initial Fock states. Moreover, since we are interested in the non-Markovian dynamics, we look for the dynamics for times much shorter than the thermalization time. With these conditions the diagonal elements of the density matrix, up to second order in κ , are

$$\begin{aligned} \rho_{0,0}(t, \omega, \varphi) &= 1 - |\beta(\omega, \varphi, t)|^2 \\ \rho_{1,1}(t, \omega, \varphi) &= |\beta(\omega, \varphi, t)|^2 \\ \rho_{k,k}(t, \omega, \varphi) &= 0, \quad k \geq 2, \end{aligned} \quad (24)$$

while the off-diagonal elements are

$$\begin{aligned} \rho_{1,0}(t, \omega, \varphi) &= \rho_{0,1}^* = \beta(\omega, \varphi, t) \\ \rho_{2,0}(t, \omega, \varphi) &= \rho_{0,2}^* = \beta^2(\omega, \varphi, t). \end{aligned} \quad (25)$$

Similarly to the heating function calculation, the final result is obtained by averaging over the phase and frequency of the driving field. Remembering that $I(\omega)/N$ is the normalized weight in the averaging and $\langle n \rangle(t, \omega, \varphi) = |\beta(t, \omega, \varphi)|^2$, with $\langle n \rangle(t, \omega, \varphi)$ given by Eq. (17), we obtain

$$\begin{aligned} \rho_{0,0}(t) &= 1 - \frac{1}{N} \int_0^\infty d\omega \frac{1}{2\pi} \int_0^{2\pi} d\varphi I(\omega) |\beta(t, \omega, \varphi)|^2 \\ &= 1 - \langle n(t) \rangle \\ \rho_{1,1}(t) &= \frac{1}{N} \int_0^\infty d\omega \frac{1}{2\pi} \int_0^{2\pi} d\varphi I(\omega) |\beta(t, \omega, \varphi)|^2 \\ &= \langle n(t) \rangle. \end{aligned} \quad (26)$$

Since we know that the heating function of the simulator matches the one of the damped harmonic oscillator we can conclude that the diagonal elements given by Eq. (26) coincide with Eq. (15). In order to prove that the state of the simulator is the time dependent thermal state of Eq. (14), now we have to prove that the out of diagonal elements are equal to zero.

The phase dependence of $\rho_{1,0}(t, \omega, \varphi)$ appears in the exponentials $\exp(\pm i\varphi)$, see Eq. (21). Averaging over the phase therefore gives

$$\rho_{1,0}(t) \propto \int_0^{2\pi} e^{\pm i\varphi} d\varphi = 0. \quad (27)$$

It is worth reminding that Eq. (9) describes the non-Markovian dynamics of the damped harmonic oscillator in the secular approximation. The same approximation in the simulator case amounts at averaging to zero the rapidly oscillating terms appearing in $\rho_{2,0}(t)$, see Appendix B. Therefore, in the secular approximation, $\rho_{2,0}(t) \simeq 0$. Summarizing, we have proved that, in the secular approximation, the density matrix of the simulator coincides with the density matrix of the damped harmonic oscillator.

It is worth noting that, since the density matrix of the damped harmonic oscillator and the one of the simulator approach coincide, the averaged driven closed system mimics correctly also the entropy production typical for open quantum systems. In other words, while the closed driven oscillator remains always in a pure state (no entropy production) the averaged state, i.e. the state of the simulator, is a mixed state since $\text{Tr} \rho^2 < 1$ for time $t > 0$ and allows the entropy production. To illustrate this point further, we display in Fig. 4, by using the simulator result given by Eq. (26), the von Neumann entropy of the system $S = -\text{Tr}(\rho \ln \rho)$. The oscillatory behavior of the entropy is a direct consequence of the oscillatory behavior of the heating function. For a more detailed description for the various types of heating function dynamics for engineered reservoirs, see Ref. [23].

IV. IMPLEMENTING THE SIMULATOR WITH A DRIVEN TRAPPED ION

Single trapped ions are a well known example of a realization of the quantum harmonic oscillator [9]. Recently these systems have also been exploited to demonstrate the creation of artificial engineered reservoirs for open quantum systems [18, 19]. The ability to cool the ion to its ground vibrational state and the long coherence time make this system ideal for the implementation of the quantum simulator described in this paper.

Important factors for the implementation of the quantum simulator presented here are the number and frequency range of the driving fields to be used in the experiment. Suppose now that we want to simulate the effect of non-Markovian off-resonant engineered reservoir to reveal the characteristic quantum mechanical oscillatory

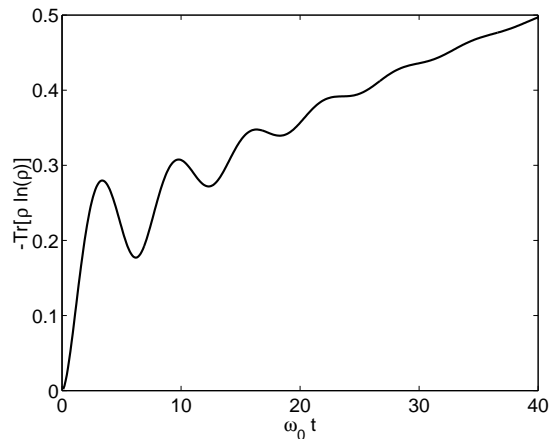


FIG. 4: The entropy production of the simulated damped oscillator in an engineered reservoir for $r = 0.1$. The oscillations of entropy directly reflect the inherent oscillatory behavior of the populations and of the heating function for the short time.

behavior of the oscillator heating function. We set the parameters to correspond to Fig. 3, $r = 0.1$, $\omega_c/2\pi = 1.1$ MHz and $k_B T/\omega_0 = 80$.

The experimental procedure is the following. We keep the step size of the frequency sampling fixed and apply a conveniently small number of pulses. We treat the phase of the field as a random variable. A typical oscillator frequency of the trapped ion in current experiments is $\omega_0/2\pi = 11$ MHz [19]. The frequency range of the periodic drive is, e.g., 0 – 12.3 MHz and the separation between the frequencies of the sets of drives is 55 kHz. In this example the total number of different applied frequencies is 225. For each frequency, the sets of different duration have to be applied in order to obtain the time evolution. The result for the heating function is obtained by converting the integral of Eq. (18) to a sum over the sets of applied electric pulses. The result of the summation has excellent agreement with the exact and theoretical quantum simulator results of Fig. 3 (d), and to avoid repetition we have not plotted in this figure the third overlapping curve. Instead it is worth mentioning that the x-axis of the figure, for the chosen experimental parameters, corresponds to μs time scale.

The system-reservoir coupling constant is directly proportional to the intensity of the applied field and the dimensionless coupling constant appearing in the analytical solution is directly given by

$$g^2 = \kappa^2 = \frac{e^2 E^2}{2m\hbar\omega_0^3}, \quad (28)$$

where E is the amplitude of the applied field and e the charge of the ion. Actually, one can choose the intensity for each set of drives ω in the most convenient way for the experimental implementation. This is because the used intensities can be rescaled when calculating the average over the frequencies for the heating function. In other words, the intensity dependence $|\alpha|^2 \propto E^2$ in Eq. (19)

stands outside the integration and can be taken outside of the corresponding summation of the experimental results. It is also worth noting that the ambient reservoir does not disturb the experiment since its effect occurs on few orders of magnitude larger time scale [9]. The vibrational quantum number of the ion can be measured in the standard way [9].

The displacement scheme presented in Sec. II has straightforward implications for interpreting the ion simulator results. A sudden switch on and off of the electric field displaces the centre of the ion trap due to interaction between the charge of the ion and the electric field. The central point is that in the adiabatic regime, the center of the trap moves slowly compared to the oscillator frequency, and the ion follows adiabatically the motion of the trap center. This effect plays a key role in the damping of the heating function in the experiment.

V. DISCUSSION AND CONCLUSIONS

In the past, the average over the stochastic fields has been used to describe the effects of ambient reservoirs to the oscillator dynamics, e.g. the heating of the ground state of trapped ions [14, 15, 16]. Here, we use similar displacement operator based formalism to investigate a new aspect to the topic. We ask the opposite question: how can controlled drives and their average be used to model the effects of a reservoir? In fact, we demonstrate how to use controlled drives to mimic the effects of both the ambient and the artificial engineered reservoirs.

In addition of the developed quantum simulator, the used approach brings to light some interesting features of the open system dynamics. We have been dealing with a characteristic quantum mechanical non-Lindblad-type master equation [23, 27]. Thus, it is somewhat surprising that the oscillations of the heating function, a typical quantum mechanical dynamical feature, have a semiclassical interpretation, when the simulator is implemented with a trapped ion. Namely, the source of the oscillations, according to our interpretation, can be seen in the “displacement-coherent state dynamics-displacement” scheme described in Sec. II. In contrast, usually the oscillatory behavior of the heating function and non-Lindblad-type-dynamics are connected to the appearance of virtual processes [23].

The results also illuminate the role of the random phase of the environment fields. In the case of oscillatory non-Markovian dynamics, the role of the random phase is to affect the amplitude of the short time oscillations. The oscillation is initiated by the low frequency fields and its amplitude is given by an average over the effects of the random phase of the same frequencies. The oscillations are then damped because of the various frequencies involved. For strictly Markovian case, the phase plays hardly any role.

Our results also shed some light on the problem of the existence of a continuous measurement scheme interpre-

tation of the quantum trajectories for non-Lindblad-type dynamics. In the Lindblad case there is a direct correspondence between the continuous measurement scheme of the environment and the quantum trajectories generated by the computer simulations [21]. For the non-Lindblad case a completely satisfactory connection is still lacking despite of some attempts [30, 31], and this important problem remains open. Thus, it is interesting to note that, in order to observe the oscillations of the heating function with the quantum simulator described here, the act of switching off the field (second displacement) has a crucial role. No measurements are allowed while the driving field is on. This points to the direction that it is probable that a satisfactory measurement scheme interpretation for non-Lindblad type dynamics does not exist, at least not in the framework of conventional quantum theory. It might be interesting to study in the future what the measurement scheme interpretations based on alternative formulations of quantum mechanics [30] would say in the context of the quantum simulator proposed here.

It is important to note that most of the existing analytical methods to study open system dynamics rely on various approximations, e.g. weak coupling between the system and the environment [10]. It would be extremely stimulating for the research on open quantum systems to possess a general quantum simulator which could be used in the regimes where most of the approximations used in the analytical calculations fail. We have taken an initial step towards this direction and a more general quantum simulator for open systems will be a challenging task for our future studies.

In conclusion, we have shown how to use a controlled driven harmonic oscillator to simulate the behavior of a damped oscillator. In other words, our results demonstrate the possibility of studying one of the paradigmatic open quantum systems models by means of a closed quantum system. Moreover, we have discussed in detail the implementation of the quantum simulator with single trapped ions. In addition, the simulator approach illuminates several interesting aspects of the non-Markovian dynamics of a damped oscillator, most notably identifying the role that the various parts of the non-Markovian spectrum play in the system dynamics.

Acknowledgments

The authors thank D. Wineland for stimulating exchange of ideas and K.-A. Suominen for illuminating discussions. This work has been supported by the Academy of Finland (projects 207614, 206108, 108699), the Magnus Ehrnrooth Foundation, and the European Union's Transfer of Knowledge project CAMEL (Grant No. MTKD-CT-2004-014427).

APPENDIX A

In this Appendix A we show that for an initial Fock state $|n=0\rangle$ the state of the system as a function of time is given by Eq. (14).

The quantum characteristic function (QCF) of the system at time t can be written [32] (for a general definition of QCF see, e.g., Ref. [33])

$$\chi_t(\xi) = e^{-\Delta_\Gamma(t)|\xi|^2} \chi_0 \left(e^{-\Gamma(t)/2} \xi \right), \quad (\text{A1})$$

where χ_0 is the QCF of the initial state of the system, and the quantities $\Delta_\Gamma(t)$ and $\Gamma(t)$ are defined in terms of the diffusion and dissipation coefficients $\Delta(t)$ and $\gamma(t)$ respectively [see master equation (9)] as follows

$$\Gamma(t) = 2 \int_0^t \gamma(t_1) dt_1, \quad (\text{A2})$$

$$\Delta_\Gamma(t) = e^{-\Gamma(t)} \int_0^t e^{\Gamma(t_1)} \Delta(t_1) dt_1. \quad (\text{A3})$$

Equation (A1) shows that the QCF is the product of an exponential factor and a transformed initial QCF.

For a Fock state $|n=0\rangle$ the initial QCF is [33]

$$\chi_0(\xi') = e^{-|\xi'|^2/2}. \quad (\text{A4})$$

By plugging Eq. (A4) into Eq. (A1) with $\xi' = e^{-\Gamma(t)/2} \xi$, the QCF at time t can be written

$$\chi_t(\xi) = \exp \left\{ - \left[\Delta_\Gamma(t) + \frac{1}{2} e^{-\Gamma(t)} \right] |\xi|^2 \right\}. \quad (\text{A5})$$

The heating function in turn, for an initial ground state of the system, can be written [23, 27]

$$\langle n(t) \rangle = \frac{1}{2} \left(e^{-\Gamma(t)} - 1 \right) + \Delta_\Gamma(t), \quad (\text{A6})$$

which gives

$$\langle n(t) \rangle + \frac{1}{2} = \Delta_\Gamma(t) + \frac{1}{2} e^{-\Gamma(t)}. \quad (\text{A7})$$

The right hand side of Eq. (A7) appears in the expression for the QCF in Eq. (A5) which can consequently be written

$$\chi_t(\xi) = \exp \left\{ - \left[\langle n(t) \rangle + \frac{1}{2} \right] |\xi|^2 \right\}. \quad (\text{A8})$$

It is also worth mentioning that for high temperature reservoir ($k_B T / \omega_0 \gg 1$) the dissipation coefficient $\gamma(t) \ll \Delta(t)$ and the heating function dynamics can be approximated with Eq. (16) [23].

The general expression for a QCF of a thermal state is [33]

$$\chi(\xi) = \exp \left\{ - \left[\bar{n} + \frac{1}{2} \right] |\xi|^2 \right\}, \quad (\text{A9})$$

where \bar{n} is the mean excitation number of the thermal state. Comparison between the QCF of the system, Eq. (A8), and the QCF of the thermal state, Eq. (A9), shows that the state of the system at each time, for the initial state we consider, is a thermal state with changing “effective” temperature given by the heating function $\langle n(t) \rangle$. Equation (14) follows then directly from this observation.

We note also that the time dependent “effective” temperature coincides with the temperature of the environment only in the long time limit when the system has reached a thermal equilibrium with its environment. It is also worth mentioning that the QCF of the thermal state with $\bar{n} = 0$, Eq. (A9), matches the QCF of the Fock state $|n = 0\rangle$, Eq. (A4), since the Fock-state $|n = 0\rangle$ coincides with the $T = 0$ thermal state.

APPENDIX B

In this Appendix B we show that in the secular approximation $\rho_{2,0}(t) \simeq 0$. From Eqs. (21) and (25) one derives

$$\rho_{2,0}(t) \propto \int_0^\infty d\omega \int_0^{2\pi} d\varphi I(\omega) [\beta_1(t, \omega, \varphi) + \beta_2(t, \omega, \varphi)]^2, \quad (\text{B1})$$

with

$$\beta_1(t, \omega, \varphi) \propto \frac{e^{-i\varphi}}{\omega + \omega_0} (e^{i\omega_0 t} - e^{-i\omega t}) \quad (\text{B2})$$

$$\beta_2(t, \omega, \varphi) \propto \frac{e^{i\varphi}}{\omega - \omega_0} (e^{i\omega t} - e^{i\omega_0 t}). \quad (\text{B3})$$

We note that

$$\begin{aligned} & \int_0^{2\pi} d\varphi [\beta_1^2(t, \omega, \varphi) + \beta_2^2(t, \omega, \varphi)] \\ &= \int_0^\pi d\varphi (c_1 e^{-2i\varphi} + c_2 e^{2i\varphi}) = 0, \end{aligned} \quad (\text{B4})$$

where $c_{1,2}$ are functions which do not depend on φ . Therefore

$$\begin{aligned} \rho_{2,0}(t) &\propto \int_0^\infty d\omega \int_0^{2\pi} d\varphi I(\omega) \beta_1(t, \omega, \varphi) \beta_2(t, \omega, \varphi) \\ &\propto \int_0^\infty d\omega I(\omega) \frac{e^{i\omega_0 t}}{\omega^2 - \omega_0^2} \sin[(\omega - \omega_0)t] \sin[(\omega + \omega_0)t] \\ &\propto e^{i\omega_0 t} \left[e^{-2\omega_c t} + \left(\frac{2i\omega_c}{\omega_0} - 1 \right) \cos(2\omega_0 t) + \frac{\omega_c}{\omega_0} \sin(2\omega_0 t) \right]. \end{aligned} \quad (\text{B5})$$

In the secular approximation, used for the study of the damped harmonic oscillator, the rapidly oscillating terms appearing in the previous equation average out to zero, as one can easily see plotting the real and imaginary part of $\rho_{2,0}(t)$.

-
- [1] M. A. Nielsen and I. L. Chuang, *Quantum Computation and Quantum Information* (Cambridge University Press, Cambridge, 2000).
 - [2] S. Stenholm and K.-A. Suominen, *Quantum Approach to Informatics* (Wiley, New York, 2005).
 - [3] P. Zoller *et al.*, Eur. Phys. J. D **36**, 203 (2005).
 - [4] A. Sørensen and K. Mølmer, Phys. Rev. Lett. **83**, 2274 (1999).
 - [5] D. Leibfried *et al.*, Phys. Rev. Lett. **89**, 247901 (2002).
 - [6] H. P. Büchler, M. Hermele, S. D. Huber, M. P. A. Fisher, and P. Zoller, Phys. Rev. Lett. **95**, 040402 (2005).
 - [7] P. M. Alsing, J. P. Dowling, and G. J. Milburn, Phys. Rev. Lett. **94**, 220401 (2005).
 - [8] M. Snoek, M. Haque, S. Vandoren, and H. T. C. Stoof, Phys. Rev. Lett. **95**, 250401 (2005).
 - [9] D. Leibfried, R. Blatt, C. Monroe, and D. Wineland, Rev. Mod. Phys. **75**, 281 (2003).
 - [10] H.-P. Breuer and F. Petruccione, *The Theory of Open Quantum systems* (Oxford University Press, Oxford, 2002).
 - [11] L. Mandel and E. Wolf, *Optical Coherence and Quantum Optics* (Cambridge University Press, Cambridge, 1995).
 - [12] I. Joichi, Sh. Matsumoto, and M. Yoshimura, Phys. Rev. A **57**, 798 (1998).
 - [13] P. Hänggi, P. Talkner, and M. Borkovec, Rev. Mod. Phys. **62**, 251 (1990).
 - [14] S. K. Lamoreaux, Phys. Rev. A **56**, 4970 (1997).
 - [15] D. F. V. James, Phys. Rev. Lett. **81**, 317 (1998).
 - [16] A. A. Budini, Phys. Rev. A **64**, 052110 (2001).
 - [17] J. F. Poyatos, J. I. Cirac, and P. Zoller, Phys. Rev. Lett. **77**, 4728 (1996).
 - [18] C. J. Myatt, B. E. King, Q. A. Turchette, C. A. Sackett, D. Kielpinski, W. M. Itano, and D. J. Wineland, Nature **403**, 269 (2000).
 - [19] Q. A. Turchette, C. J. Myatt, B. E. King, C. A. Sackett, D. Kielpinski, W. M. Itano, C. Monroe, and D. J. Wineland, Phys. Rev. A **62**, 053807 (2000).
 - [20] P. Rabl, A. Shnirman, and P. Zoller, Phys. Rev. B **70**, 205304 (2004).
 - [21] M. B. Plenio and P. L. Knight, Rev. Mod. Phys. **70**, 101 (1998), and references therein.
 - [22] C. W. Gardiner and P. Zoller, *Quantum Noise: A Handbook of Markovian and non-Markovian Quantum Stochastic Methods with Applications to Quantum Optics* (Springer-Verlag, Berlin, 1999).
 - [23] S. Maniscalco, J. Piilo, F. Intravaia, F. Petruccione, and

- A. Messina, Phys. Rev. A **70**, 032113 (2004).
- [24] F. Intravaia, S. Maniscalco, and A. Messina, Eur. Phys. J. D **32** 97 (2003).
 - [25] A. O. Caldeira and A. J. Leggett, Physica A **121**, 587 (1983).
 - [26] U. Weiss, *Quantum Dissipative Systems* (World Scientific Publishing, Singapore, 1999).
 - [27] S. Maniscalco, J. Piilo, F. Intravaia, F. Petruccione, and A. Messina, Phys. Rev. A **69**, 052101 (2004).
 - [28] The physical explanation of the oscillations of the heating function in the non-Markovian regime [Fig. 3 (d)] is the virtual exchange of energy between the system and the environment. These have been studied in more detail in Ref. [23].
 - [29] F. Intravaia, S. Maniscalco, J. Piilo, and A. Messina, Phys. Lett. A **308**, 6 (2003).
 - [30] J. Gambetta and H. M. Wiseman, Phys. Rev. A **68**, 062104 (2003).
 - [31] H.-P. Breuer, Phys. Rev. A **70**, 012106 (2004).
 - [32] F. Intravaia, S. Maniscalco, and A. Messina, Phys. Rev. A **67**, 042108 (2003).
 - [33] S. M. Barnett and P. M. Radmore, *Methods in Theoretical Quantum Optics* (Oxford University Press, Oxford, 1997).